

Marquette University
e-Publications@Marquette

Chemistry Faculty Research and Publications

Chemistry, Department of

4-1-2010

Synergistic Effect of Carbon Nanotubes and Decabromodiphenyl Oxide/Sb₂O₃ in Improving the Flame Retardancy of Polystyrene

Hongdian Lu
Marquette University

Charles A. Wilkie
Marquette University, charles.wilkie@marquette.edu

Accepted version. *Polymer Degradation and Stability*, Vol. 95, No. 4 (April 2010): [DOI](#). © 2010 Elsevier. Used with permission.

NOTICE: this is the author's version of a work that was accepted for publication in *Polymer Degradation and Stability*. Changes resulting from the publishing process, such as peer review, editing, corrections, structural formatting, and other quality control mechanisms may not be reflected in this document. Changes may have been made to this work since it was submitted for publication. A definitive version was subsequently published in *Polymer Degradation and Stability*, VOL 95, ISSUE 4, April 2010, [DOI](#).

Synergistic Effect of Carbon Nanotubes and Decabromodiphenyl Oxide/Sb₂O₃ for Improving the Flame Retardancy of Polystyrene

Hongdian Lu

State Key Laboratory of Fire Science, University of Science and Technology of China

Hefei, Anhui 230026, PR China

Department of Chemical and Materials Engineering, Hefei University

Hefei, Anhui 230022, PR China.

Charles A. Wilkie

Department of Chemistry and Fire Retardant Research Facility, Marquette University

Milwaukee, WI

Abstract:

Brominated flame retardant polystyrene composites were prepared by melt blending polystyrene, decabromodiphenyl oxide, antimony oxide, multi-wall carbon nanotubes and montmorillonite clay. Synergy between carbon nanotubes and clay and the brominated fire retardant was studied by thermogravimetric analysis, microscale combustion calorimetry and cone calorimetry. Nanotubes are more efficient than clay in improving the flame

retardancy of the materials and promoting carbonization in the polystyrene matrix. Comparison of the results from the microscale combustion calorimeter and the cone calorimeter indicate that the rate of change of the peak heat release rate reduction in the microscale combustion calorimeter was slower than that in the cone. Both heat release capacity and reduction in the peak heat release rate in the microscale combustion calorimeter are important for screening the flame retardant materials; they show good correlations with the cone parameters, peak heat release rate and total heat released.

Keywords: Polystyrene, Clay, Carbon nanotubes, Microscale combustion calorimeter, Flame retardant.

1. Introduction

Polystyrene (PS) is a widely used but easily burned polymer and thus it is necessary to improve its flame retardancy. Combinations of nanoparticles, such as organically modified montmorillonite clay, with traditional flame retardants, including halogen-free flame retardants, brominated flame retardant and intumescent flame retardants, have exhibited good flame retardant synergy and improved comprehensive properties while overcoming the limitation of the traditional flame retardants, such as the required high loading [1], [2], [3], [4], [5] and [6]. In addition to clay, carbon nanotubes (CNT) are another nanoscale candidate as a flame retardant adjunct for fire-resistant polymeric materials. CNT exhibited better efficiency than clay in reducing peak heat release rate for polymers such as ethylene vinyl acetate (EVA) and acrylonitrile-butadiene-styrene (ABS) as tested by the cone calorimeter, mainly due to the formation of an entangled fiber network in the condensed phase and only minimal addition was required (<5%) [7], [8], [9], [10], [11], [12] and [13].

Recently, microscale combustion calorimetry (MCC) has been developed as high-throughput method for the formulation and flammability screening of multi-component polymeric materials. Compared with conventional fire testing techniques, such as limiting oxygen index (LOI), UL-94 vertical combustion tests and cone calorimetry (Cone), MCC can quickly and easily obtain the key flammability parameters of the materials from just a few milligrams instead of tens or more grams of specimen [14], [15], [16] and [17]. In some cases, MCC results have been shown to correctly predict the results of other fire tests, but this is not always the case.

In the paper, bromine-antimony oxide (Sb_2O_3) flame retardant PS composites with multi-wall nanotubes (MWNT) and montmorillonite clay were prepared and the combination of the flame retardant additives with MWNT or clay to improve the flame retardancy of PS composites was investigated. An important aim of this work is to compare the parameters related to fire risk from MCC and Cone tests to establish the relationship between them.

2. Experimental

2.1. Materials

Polystyrene (PS, $M_w \sim 192000$, melt index 6.00–9.00 g/10 min (200 °C/5.0 kg, ASTM D1238)) was purchased from Aldrich Chemical Co. Organically modified montmorillonite clay (Cloisite15A (cation is dimethyldihydrogenated tallow ammonium), Southern Clay Products), decabromodiphenyl oxide (Deca, SAYTEX 102E, theoretical bromine content $\sim 83.3\%$, Albemarle Co.), antimony oxide (AO, Laurel industries) and multi-wall carbon nanotubes (MWNT, Nanocyl, S.A, Belgium) were all used as received.

2.2. Preparation

The brominated flame retardant PS composites with and without MWNT or clay were melt compounded using a Brabender mixer at 180 °C for 10 min at a screw speed of 60 rpm. The ratio of Deca/AO (abbreviated as BFR) was fixed as 5/1 by weight and the formulations are given in Table 1.

2.3. Characterization

Thermogravimetric analyses (TGA) were conducted with a Netzsch TG209 F1 thermoanalyzer instrument. Specimens with mass of 15 ± 1 mg were heated from 30 to 700 °C at a heating rate of 20 °C/min in a nitrogen atmosphere at a flow rate of 40 ml/min. All samples were run in duplicate and the average values are reported; the temperature is reproducible to ± 1 °C and the mass to $\pm 0.2\%$.

Pyrolysis combustion flow calorimetry experiments were carried out on a Govmark MCC-2 microscale combustion calorimeter (MCC).

Samples weighing 4 ± 1 mg were heated to 750 °C at a ramp rate of 1 °C/s in a stream of nitrogen flowing at 80 ml/min. The combustor temperature was set at 900 °C and oxygen/nitrogen flow rate was set at 20/80 ml/ml. The reported data are averages of three measurements and the typical relative error for heat release capacity is $\pm 10\%$.

The cone calorimeter experiments were carried out using an Atlas Cone 2 instrument according to ASTM E 1354, on 3 mm thick 100×100 mm² plaques. All samples were tested in triplicate. The cone data obtained are reproducible to within $\pm 10\%$ when measured at a heat flux of 35 kW/m².

3. Results and discussion

3.1. Thermal degradation stability

Fig. 1 gives the thermogravimetric analysis (TGA) and derivative TGA (DTG) curves for the brominated flame retardant PS composites. The data for the temperature at which 5% ($T_{5\%}$) and 50% ($T_{50\%}$) thermal degradation occurs, and the temperature of the first and second maximum mass loss rate ($T_{1\max}$ and $T_{2\max}$) obtained from the DTG curves, are listed in Table 1. The TGA curves display a one-step degradation process for pure PS but a two-stage process for PS/BFR composites, except for sample PS/BFR-7 which has the largest amount of BFR. Increasing the BFR content leads to small change in the temperature at which $T_{1\max}$ occurs in the range 375–385 °C, while $T_{2\max}$ decreases by about 20 °C, suggesting that BFR destabilizes PS. As shown in Fig. 1(b), the first peak of mass loss rate for PS/BFR samples increases sharply with increasing BFR content due to chemical reaction between Deca and Sb₂O₃ to generate gas-phase flame retardants, which are expected to retard the mass loss rate at higher temperature.

The partial replacement of BFR by MWNT, clay or MWNT/clay combinations at the same total loading of 12% for BFR + MWNT (clay), results in the deterioration of the thermal stability in terms of $T_{5\%}$, but an increase in char formation at 600 °C. Although both clay and MWNT have carbonization effect on PS/BFR composites, as compared in Table 1, the char increases in the order

clay < clay/MWNT < MWNT for the samples PS/BFR/clay2.0, PS/BFR/clay1.0/MWNT1.0 and PS/BFR/MWNT2.0, which indicates that MWNT can offer more advantage in carbonization than clay. Meanwhile, the introduction of 2% clay or MWNT/clay combinations are more efficient in lowering the first mass loss rate than either PS/BFR-5 or PS/BFR/MWNT2.0, but $T_{1\max}$ shows about a 30 °C decrease (Fig. 2, Table 1).

3.2. MCC studies

The microscale combustion calorimeter (MCC) based on oxygen consumption calorimetry is also known as pyrolysis combustion flow calorimetry (PCFC). By directly measuring the heat of combustion of the gases evolved during controlled heating of 0.5–50 mg samples, fire parameters can be obtained. Fig. 3 shows the heat release rate curves from the MCC (HRR-MCC) compared to the DTG curves for selected samples, PS/BFR-5, PS/BFR/clay2.0, PS/BFR/MWNT2.0 and PS/BFR/MWNT1.0/clay1.0. For the PS/BFR systems showing two degradation steps in DTG, only one HRR-MCC peak shifted to higher temperature was observed in the MCC curve (Fig. 3a). When clay, MWNT and MWNT/clay were introduced into PS/BFR system, two or more peaks are found in the MCC curve (Fig. 3b–d). Meanwhile, PS/BFR-5 and PS/BFR/MWNT2.0 have the same onset degradation temperature (T_{onset}) in MCC as the DTG (Fig. 3a, c), while samples containing clay (Fig. 3b, d), PS/BFR/clay2.0 and PS/BFR/MWNT1.0/clay1.0, show delayed T_{onset} in MCC compared to the DTG. Perhaps these differences are due to the higher heating rate in the MCC (1 °C/s (60 °C/min) for MCC vs 20 °C/min for TGA), and may indicate that clay is more efficient in protecting specimens from degradation than MWNT in MCC tests.

The primary parameters obtained by MCC are peak heat release rate (PHRR-MCC), heat release capacity (HRC-MCC), total heat released (THR-MCC) and temperature at PHRR (T_p -MCC) (Table 2). A comparison of HRC-MCC, THR-MCC and T_p -MCC are shown in Fig. 4. For the PS/BFR systems (Fig. 4a), one can note a decrease in the THR-MCC with increasing BFR content and there is a high correlation (correlation coefficient, $R = 0.98$) between them. However, there is not a correlation between HRC-MCC and BFR content. HRC-MCC decreases sharply with initial increasing BFR content to 3.6% then

decreases slightly at higher loading. A similar tendency has been found in PHRR-MCC. Comparisons of the results for the samples with 12% additives from Fig. 4(b–d) confirm that the introduction of clay or MWNT into the BFR is of benefit to reducing HRC-MCC and THR-MCC while enhancing T_p -MCC for the materials. Moreover, it is noted that HRC-MCC appears to have no correlation with all flame retardant formulations. When the degradation occurs in a single step, the HRC-MCC can be easily obtained, however when the degradation involves multiple steps, one may sum the values or average them and it is not yet known how this is best accomplished for any system [16].

As reported by Lewin, synergistic effectivity (SE) in flame retardant polymeric materials, which is considered the tool to characterize and compare synergistic systems, can be defined as the ratio of the flame retardant effectivity (EFF) of flame retardant additives plus the synergist to that of the additives without synergist, where the EFF was calculated by the increase of LOI for 1 wt% of the flame retardant element [18] and [19]. In this paper, the concept of EFF and SE is used to identify the synergistic effect of the various additives on brominated flame retardant PS, where the EFF is defined as the decrease of peak HRR obtained from MCC (PHRR-MCC) and peak HRR obtained from cone calorimeter (PHRR-Cone) for 1 wt% of the flame retardant element bromine (Br) in MCC and Cone tests, respectively. A summary of the EFF and SE of the bromine flame retardant PS formulations with 12 wt% additives is tabulated in Table 3. The results indicate that AO/clay, AO/MWNT and AO/MWNT/clay have a substantially higher SE than does AO alone.

3.3. Cone calorimetric studies

The cone calorimeter is one of the most effective bench-scale methods to study the flammability properties of materials; the parameters that are available include the heat release rate and especially its peak value (PHRR-Cone); the total heat released (THR-Cone); the average effective heat of combustion (AEHC-Cone); the average mass loss rate (AMLR-Cone); the time to ignition (t_{ign} -Cone) and the time to PHRR (t_p -Cone); finally one can derive two parameters from cone data, the fire performance index (FPI-Cone, defined as t_{ign} -Cone divided by PHRR-Cone) and the fire growth rate (FIGRA-Cone, defined as PHRR-Cone divided by t_p -Cone).

The heat release rate, in particular peak HRR, has been found to be the most important parameter to evaluate fire safety. Fig. 5 and Table 4 give plots and combustion data in the cone calorimeter for PS/BFR with and without MWNT or clay. The dynamic HRR-Cone curves of various BFR loadings from samples PS/BFR-1 to 7 are shown in Fig. 5(a). Pure PS burned rapidly after ignition and a HRR-Cone peak appeared at 180s. When BFR is present, $t_{\text{ign-Cone}}$ of PS/BFR samples increased slightly with a decline of PHRR-Cone and t_p -Cone. Higher BFR loading (PS/BFR-7), however, shows no additional benefit in further reducing the flammability properties in terms of PHRR-Cone, there is a maximum effective content of BFR that is needed. The data listed in Table 4 show that THR-Cone and AEHC-Cone of the series of samples is reduced as the BFR content increases. Increased AEHC-Cone is the response of the combustion of combustible gases in the gas phase; the lower AEHC-Cone corresponding to a higher BFR content confirms the existence of a gas-phase flame retardant mechanism. Clearly, all PS/BFR samples show higher average specific extinction area (ASEA-Cone, a measure of the smoke yield) than PS, caused by the bromine-containing radicals terminating the active radicals in the burning gas phase, resulting in incomplete combustion of the pyrolysis products from PS thus giving more smoke. The replacement of BFR by clay or MWNT leads to different HRR-Cone features compared to PS/BFR-5. As shown in Fig. 5(b), these samples ignite earlier but burn more slowly than PS/BFR-5, resulting in a 42% reduction in PHRR-Cone from 591 for PS/BFR-5 to about 340 kW/m² for 2 and 3% MWNT containing samples.

The synergistic effectivity of nanoparticles-BFR system in flame retardant PS composites tested by Cone is similar to that tested by MCC, as listed in Table 3. The SE values for Cone are a little different than those from MCC but the trend is obvious. The advantage in improving flame retardancy by the introduction of clay to the bromine-Sb₂O₃ system is believed to be due to the concurrent existence of chemical reactivity and physical effects. That is, the products from Hoffman degradation of clay react with BFR, promoting the generation of SbBr₃ and SbBr₃-RNH₃Br complexes as efficient gas-phase fire retardants [1] and [2]. Meanwhile, the barrier (the physical effect) formed from the nano-dispersed silicate layers can further protect the substrate from fire. As a result, the material will exhibit reduced PHRR-Cone, lower AMLR-Cone and decreased t_{ign} .

It is noted that PS/BFR/MWNT2.0 shows higher SE in reducing PHRR-Cone than PS/BFR/clay2.0; two things are postulated to be responsible for the difference. The first is that the barrier efficiency of PS/BFR/MWNT2.0 induced by the formation of a structured-network in the condensed phase during the burning of the PS/CNT is higher than that of polymer/clay nanocomposites. Photographs of the residual char in PS/BFR/clay2.0 and PS/BFR/MWNT2.0 after cone tests are shown in Fig. 6 and give further evidence that the later leaves a heavier integrated char covering all the surface of the aluminum container, while only a few island-like char particles are observed in the former at the end of the test. The second item to be considered is the catalytic activity of MWNT. Since the MWNT used was not purified, trace transition metals, such as Fe and Co supported on Al₂O₃ as catalyst, will be retained in MWNT during the preparation. These particles may catalyze the degradation of PS by dehydrogenation to participate in the carbonization process to form char, in agreement with the result from TGA that more char is produced from the CNT-containing material [20] and [21]. Meanwhile, these metals can trap radicals such as H• and HO• in the burning gas phase and lead to flame extinguishment [22]. As confirmed in Table 3, PS/BFR/WMNT2.0 shows higher ASEA-Cone than PS/BFR/clay2.0, attributed to the incomplete combustion of the pyrolysis products of PS.

4. Correlation between cone and MCC

Microscale combustion calorimetry (MCC) has been accepted as a new screening method to measure fire performances of flame retardant materials using a few milligrams of specimen. Each of the MCC data, namely HRC-MCC, THR-MCC, char yield and T_p -MCC, have been taken into consideration and correlate reasonably with the conventional flame retardant test results such as cone calorimetry, limiting oxygen index (LOI) and UL-94 classification in different polymer matrices [23], [24] and [25].

In this investigation, correlation coefficients, R , between MCC and Cone data calculated by Minitab 15 Statistical Software for the 13 formulations are tabulated in Table 5, and those showing high correlation coefficients ($IRI \geq 0.80$) are highlighted in bold and italics. Although all the filled samples exhibit lower PHRR values in both the MCC and Cone than does pure PS, the changes in the PHRR reduction

upon addition of the additives are different. As shown in Fig. 7(a), PS formulations with BFR less than 10% exhibit much higher PHRR reductions in the MCC (Reduct-MCC) than in the Cone (Reduct-Cone). However, a good correlation, $R = 0.875$, between Reduct-MCC and Reduct-Cone has been found in Fig. 7(b). Meanwhile, Fig. 7(c) demonstrates that the low HRC-MCC values correspond to the low PHRR-Cone. As listed in Table 5, HRC-MCC is highly correlated with PHRR-Cone, THR-Cone, AEHC-Cone and Reduct-Cone, but poorly with other parameters including AMLR, t_{ign} , FPI and FIGRA. Moreover, Reduct-MCC shows similar correlation with Cone parameters as HRC-MCC.

5. Conclusions

Thermal and flammability performance of brominated flame retardant PS composites with clay or MWNT have been investigated. Synergy between BFR and MWNT is higher than that between BFR and clay in improving flame retardancy in both MCC and Cone tests. MWNT can promote the participation of polymer chains in the carbonization process and generate increased char yield. Although the materials are more fire safe, the time to ignition is decreased. Relationships between MCC and Cone suggest good correlations between both HRC and PHRR reduction in MCC with PHRR-Cone, THR-Cone and PHRR reduction. Since the reduction of the heat release rate measured by the cone calorimeter is the most clear-cut evidence for the efficiency of flame retardants, MCC, as a high-throughput method, can provide this information on a much smaller sample and in much less time for PS with brominated flame retardants.

Acknowledgements

The work was partially financially supported by the US Air Force under grant number FA8650-07-1-5901, the Program for Specialized Research Fund for the Doctoral Program of Higher Education (200803580008), the Program for Science and Technology of SuZhou (SG-0841), the National Natural Science Foundation of China (No. 50903080) and China Postdoctoral Science Foundation (20080430101).

References

1. Zanetti M, Camino G, Canavese D, Morgan AB, Lamelas FJ, Wilkie CA. Fire retardant halogen-antimony-clay synergism in polypropylene layered silicate nanocomposites. *Chem Mater* 2002;14(1):189-93.
2. Wang DY, Echols K, Wilkie CA. Cone calorimetric and thermogravimetric analysis evaluation of halogen-containing polymer nanocomposites. *Fire Mater* 2005;29(5):283-94.
3. Hu Y, Wang SF, Ling ZH, Zhuang YL, Chen ZY, Fan WC. Preparation and combustion properties of flame retardant nylon 6/montmorillonite nanocomposite. *Macromol Mater Eng* 2003;288(3):272-6.
4. Morgan AB. Flame retarded polymer layered silicate nanocomposites: a review of commercial and open literature systems. *Polym Adv Technol* 2006;17(4):206-17.
5. Song L, Hu Y, Lin Z, Xuan SY, Wang SF, Chen ZY, et al. Preparation and properties of halogen-free flame-retarded polyamide 6/organoclay nanocomposite. *Polym Degrad Stab* 2004;86:535-40.
6. Hu Y, Tang Y, Song L. Poly(propylene)/clay nanocomposites and their application in flame retardancy. *Polym Adv Technol* 2006;17(4):235-45.
7. Kashiwagi T, Grulke E, Hilding J, Groth K, Harris R, Butler K, et al. Thermal and flammability properties of polypropylene/carbon nanotube nanocomposites. *Polymer* 2004;45(12):4227-39.
8. Ma HY, Tong LF, Xu ZB, Fang ZP. Functionalizing carbon nanotubes by grafting on intumescent flame retardant: nanocomposite synthesis, morphology, rheology, and flammability. *Adv Fun Mater* 2008;18(3):414-21.
9. Peeterbroeck S, Laoutid F, Swoboda B, Lopez-Cuesta JM, Moreau N, Nagy JB, et al. How carbon nanotube crushing can improve flame retardant behaviour in polymer nanocomposites? *Macromol Rapid Commun* 2007;28(3):260-4.
10. Gao FG, Beyer G, Yuan QC. A mechanistic study of fire retardancy of carbon nanotube/ethylene vinyl acetate copolymers and their clay composites. *Polym Degrad Stab* 2005;89(3):559-64.

11. Ma HY, Tong LF, Xu ZB, Fang ZP. Synergistic effect of carbon nanotube and clay for improving the flame retardancy of ABS resin. *Nanotechnology* 2007;18(37):1-8.
12. Costache MC, Wang DY, Heidecker MJ, Manias E, Wilkie CA. The thermal degradation of poly(methyl methacrylate) nanocomposites with montmorillonite, layered double hydroxides and carbon nanotubes. *Polym Adv Technol* 2006;17(4):272-80.
13. Marosfoi BB, Marosi GJ, Szep A, Anna P, Keszei S, Nagy BJ, et al. Complex activity of clay and CNT particles in flame retarded EVA copolymer. *Polym Adv Technol* 2006;17(4):255-62.
14. Hergenrother PM, Thompson CM, Smith JG, Connell JW, Hinkley JA, Lyon RE, et al. Flame retardant aircraft epoxy resins containing phosphorus. *Polymer* 2005;46(14):5012-24.
15. Walters RN, Lyon RE. Molar group contributions to polymer flammability. *J Appl Polym Sci* 2003;87(3):548-63.
16. Schartel B, Pawlowski KH, Lyon RE. Pyrolysis combustion flow calorimeter: a tool to assess flame retarded PC/ABS materials? *Thermochim Acta* 2007;462(1-2):1-14.
17. Lyon RE, Walters RN, Stoliarov SI. Screening flame retardants for plastics using microscale combustion calorimetry. *Polym Eng Sci* 2007;47(10):1501-10.
18. Lewin M. Synergism and catalysis in flame retardancy of polymers. *Polym Adv Technol* 2001;12:215-22.
19. Lewin M. Synergistic and catalytic effects in flame retardancy of polymeric materials—an overview. *J Fire Sci* 1999;17:3-17.
20. Kim JS, Lee WY, Lee SB, Kim SB, Choi MJ. Degradation of polystyrene waste over base promoted Fe catalysts. *Catal Today* 2003;87(1-4):59-68.
21. Xi GX, Rui L, Tang QH, Li JH. Mechanism studies on the catalytic degradation of waste polystyrene into styrene in the presence of metal powders. *J Appl Polym Sci* 1999;73(7):1139-43.
22. Kong QH, Lv RB, Zhang SJ. Flame retardant and the degradation mechanism of high impact polystyrene/Fe-montmorillonite nanocomposites. *J Polym Res* 2008;15:453-8.

23. Cogen JM, Lin TS, Lyon RE. Correlations between pyrolysis combustion flow calorimetry and conventional flammability tests with halogen-free flame retardant polyolefin compounds. *Fire Mater* 2009;33(1):33-50.
24. Schall FP, Morgan AB. Microcombustion calorimetric measurements of flame retardant plastics. *Polym Mater Sci Eng* 2008;98:252-3.
25. Morgan AB, Galaske ML. Microcombustion calorimetry screening of non-halogenated flame retardant polymer-clay/polymer-nanofiber composites. *Polym Mater Sci Eng* 2008;98:248-9.

About the Authors

Charles A. Wilkie : Department of Chemistry and Fire Retardant Research Facility, Marquette University, P.O. 1881, Milwaukee, WI 53201-1881, USA.

Tel.: +1 414 288 7239; fax: +1 414 288 7066.

Email: charles.wilkie@marquette.edu

Appendix

Table 1: Compositions and TGA data of brominated flame retardant PS composites (average values).

Sample	Composites (%)				TGA				
	PS	BFR (Deca/AO = 5/1)	MWNT	OMT	$T_{5\%}$ (°C)	$T_{50\%}$ (°C)	Char (% 600 °C)	T_{1max} (°C)	T_{2max} (°C)
Pure PS	100				378	415	/	421	
PS/BFR-1 (A1)	98.8	1.2			372	417	0.5	385	425
PS/BFR-2 (A2)	96.4	3.6			367	411	0.6	378	420
PS/BFR-3 (A3)	94	6.0			364	403	1.3	376	412
PS/BFR-4 (A4)	90.4	9.6			363	399	1.3	377	411
PS/BFR-5 (A5)	88	12			363	398	2.2	378	407
PS/BFR-6 (A6)	82	18			364	394	3.3	381	403
PS/BFR-7 (A7)	76	24			362	390	4.4	382	
PS/BFR/MWNT0.5 (B1)	88	11.5	0.5		358	398	3.1	378	409
PS/BFR/MWNT2.0 (B2)	88	10	2		361	403	4.6	372	413
PS/BFR/MWNT3.0 (B3)	88	9	3		359	405	4.7	381	413
PS/BFR/clay2.0 (C1)	88	10		2	333	398	2.5	347	410
PS/BFR/clay1.0/MWNT1.0 (D1)	88	10	1	1	339	401	2.9	352	413

$T_5\%$, temperature at which 5% degradation occurs; $T_{50\%}$, temperature at which 50% degradation occurs; T_{1max} and T_{2max} , temperature obtained from DTG curves at which the maximum mass loss rate occurs during the first and second step; Char, the fraction of the residue remaining at 600 °C.

Table 2: MCC data of brominated flame retardant PS composites.

Sample	PHRR (W/g)	HRC (J/g k)	THR (kJ/g)	T _p (°C)	Reduct- MCC (%)
Pure PS	1046 ± 8	1026 ± 8	38 ± 0	441 ± 1	0
PS/BFR-1	797 ± 49	785 ± 51	38 ± 0	435 ± 3	24
PS/BFR-2	561 ± 36	582 ± 16	38 ± 0	434 ± 5	46
PS/BFR-3	605 ± 19	596 ± 22	35 ± 0	410 ± 3	42
PS/BFR-4	567 ± 19	578 ± 39	34 ± 1	421 ± 1	46
PS/BFR-5	598 ± 26	586 ± 26	33 ± 0	409 ± 7	43
PS/BFR-6	487 ± 17	489 ± 1	28 ± 1	417 ± 2	53
PS/BFR-7	472 ± 7	463 ± 6	24 ± 0	408 ± 1	55
PS/BFR/MWNT0.5	545 ± 13	552 ± 12	32 ± 0	407 ± 1	48
PS/BFR/MWNT2.0	341 ± 11	431 ± 4	31 ± 0	429 ± 2	67
PS/BFR/MWNT3.0	419 ± 68	445 ± 3	32 ± 0	428 ± 3	60
PS/BFR/clay2.0	408 ± 51	401 ± 50	33 ± 1	432 ± 2	61
PS/BFR/clay1.0/MWNT1.0	438 ± 9	432 ± 11	33 ± 0	430 ± 4	58

PHRR, peak heat release rate; HRC, heat release capacity; THR, total heat released; T_p, temperature at PHRR; Reduct-MCC, $100 \times (\text{PHRR}_{\text{polymer}} - \text{PHRR}_{\text{composite}}) / \text{PHRR}_{\text{polymer}}$.

Table 3: Flame retardant effectivity (EFF) and synergistic effectivity (SE) of brominated flame retardant PS tested by MCC and Cone.

Samples	Flame retardant (Br content,%)	Synergists	MCC			Cone		
			PHRR	EFF	SE	PHRR	EFF	SE
PS	/	/	1046	/	/	1166	/	/
PS/Deca ^a	Deca (10.0)	/	766	28	/	799	37	/
PS/BFR-5	Deca (8.3)	AO	598	54	1.9	591	69	1.9
PS/BFR/clay2.0	Deca (6.9)	AO + clay	408	92	3.3	442	105	2.8
PS/BFR/MWNT2.0	Deca (6.9)	AO + MWNT	341	102	3.6	340	120	3.2
PS/BFR/clay1.0/MWNT1.0	Deca (6.9)	AO + clay + MWNT	438	88	3.1	381	114	3.1

EFF, flame retardant effectivity, $(\text{PHRR}_{\text{polymer}} - \text{PHRR}_{\text{composite}}) / \text{Br content}$; SE, synergistic effectivity, $\text{EFF}_{\text{Deca+Synergists}} / \text{EFF}_{\text{Deca}}$.

^a The ratio of PS/Deca is 88/12 by weight.

Table 4: Cone data of brominated flame retardant PS composites.

Sample	PHRR (kW/m ²)	t _p (s)	THR (MJ/m ²)	AEHC (MJ/kg)	ASEA (m ² /kg)	AMLR (g/m ² s)	t _{ign} (s)	FPI	FIGRA	Reduct-Cone (%)
Pure PS	1166 ± 93	180 ± 14	101 ± 5	28 ± 6	1008 ± 221	27 ± 2	44 ± 10	0.04 ± 0.01	6.5 ± 0.1	0
PS/BFR-1	1123 ± 80	172 ± 7	94 ± 2	31 ± 1	1269 ± 145	27 ± 2	42 ± 2	0.01 ± 0.02	2.2 ± 3.8	4
PS/BFR-2	958 ± 30	107 ± 7	74 ± 3	24 ± 1	1502 ± 51	28 ± 3	46 ± 4	0.05 ± 0.03	9.0 ± 0.8	18
PS/BFR-3	808 ± 92	115 ± 6	58 ± 3	20 ± 2	1801 ± 101	29 ± 2	51 ± 4	0.06 ± 0.01	7.0 ± 0.8	31
PS/BFR-4	784 ± 93	128 ± 3	51 ± 1	17 ± 1	1976 ± 25	31 ± 1	54 ± 2	0.07 ± 0.01	6.1 ± 0.6	33
PS/BFR-5	591 ± 32	128 ± 2	46 ± 1	15 ± 0	2159 ± 100	31 ± 3	55 ± 2	0.09 ± 0.01	4.6 ± 0.3	49
PS/BFR-6	509 ± 18	113 ± 17	40 ± 3	12 ± 2	1843 ± 244	27 ± 5	53 ± 8	0.10 ± 0.01	4.5 ± 0.6	56
PS/BFR-7	590 ± 13	105 ± 6	39 ± 1	9 ± 0	1195 ± 49	27 ± 1	52 ± 6	0.06 ± 0.05	3.8 ± 3.3	49
PS/BFR/MWNT0.5	455 ± 32	108 ± 6	40 ± 3	10 ± 4	1646 ± 85	28 ± 3	29 ± 4	0.04 ± 0.04	2.8 ± 2.5	61
PS/BFR/MWNT2.0	340 ± 11	141 ± 2	43 ± 2	15 ± 0	2373 ± 98	23 ± 1	34 ± 2	0.10 ± 0.05	2.4 ± 0.1	71
PS/BFR/MWNT3.0	339 ± 13	117 ± 11	45 ± 1	15 ± 1	2325 ± 42	26 ± 6	38 ± 1	0.11 ± 0.04	2.9 ± 0.2	71
PS/BFR/clay2.0	442 ± 32	115 ± 2	43 ± 3	13 ± 0	1943 ± 8	24 ± 5	35 ± 4	0.05 ± 0.05	2.6 ± 2.2	62
PS/BFR/clay1.0/MWNT1.0	381 ± 33	131 ± 1	43 ± 1	15 ± 1	2213 ± 55	24 ± 0	30 ± 3	0.08 ± 0.01	2.9 ± 0.3	67

PHRR, peak heat release rate; t_p, time to peak heat release rate; THR, total heat released; AEHC, average effective heat of combustion; ASEA, average specific extinction area; AMLR, average mass loss rate; t_{ign}, time to ignition; FPI, fire performance index, t_{ign}/PHRR; FIGRA, fire growth rate, PHRR/t_p; Reduct-Cone, 100 × (PHRR_{polymer} - PHRR_{composite})/PHRR_{polymer}.

Table 5: Correlation coefficients between MCC and Cone data for brominated flame retardant PS composites.

	HRC-MCC	THR-MCC	Reduct-MCC	PHRR-Cone	t _p -Cone	THR-Cone	AEHC-Cone	AMLR-Cone	t _{ign} -Cone	FPI-Cone	FIGRA-Cone	Reduct-Cone
HRC-MCC	*											
THR-MCC	0.636	*										
Reduct-MCC	-0.991	-0.641	*									
PHRR-Cone	0.872	0.662	-0.876	*								
t _p -Cone	0.767	0.557	-0.727	0.577	*							
THR-Cone	0.901	0.765	-0.882	0.917	0.766	*						
AEHC-Cone	0.793	0.840	-0.766	0.865	0.747	0.959	*					
AMLR-Cone	0.330	0.173	-0.366	0.436	-0.149	0.131	0.116	*				
t _{ign} -Cone	0.221	-0.106	-0.254	0.408	-0.086	0.110	0.104	0.725	*			
FPI-Cone	-0.593	-0.482	0.621	-0.719	-0.374	-0.659	-0.565	-0.158	0.076	*		
FIGRA-Cone	0.382	0.401	-0.386	0.579	-0.105	0.385	0.374	0.581	0.572	-0.134	*	
Reduct-Cone	-0.872	-0.662	0.875	-1.000	-0.577	-0.917	-0.866	-0.435	-0.409	0.719	-0.579	*

Fig. 1.: TGA and DTC curves of PS/BFR composites at 20 °C/min in a N2 atmosphere.

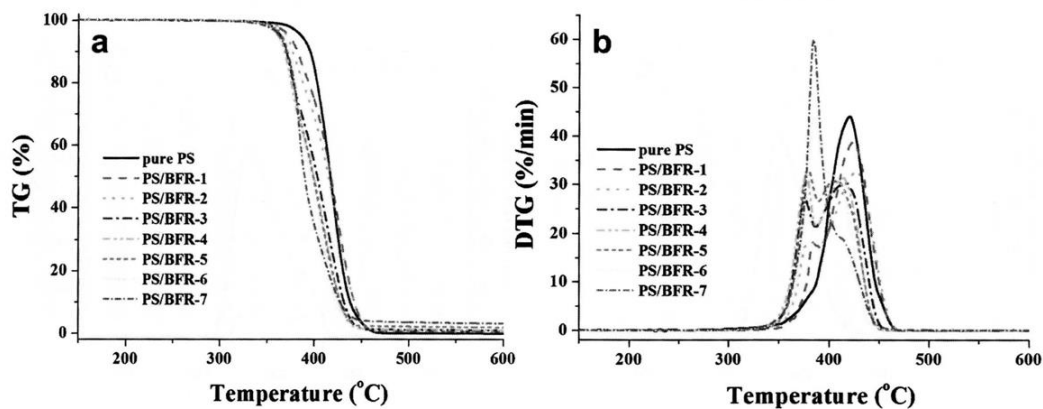


Fig. 2.: TGA and DTG curves of PS/BFR composites with clay and MWNT.

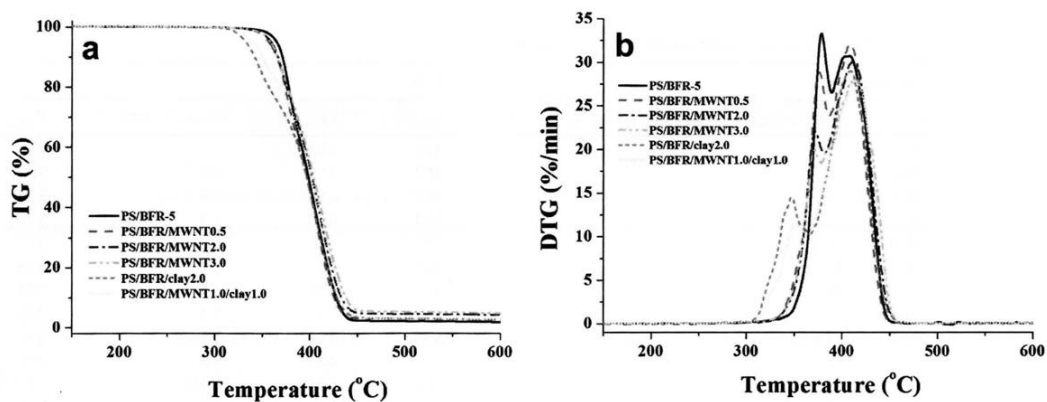


Fig. 3.: Comparison of MCC and DTGA curves for PS composites with various formulations.

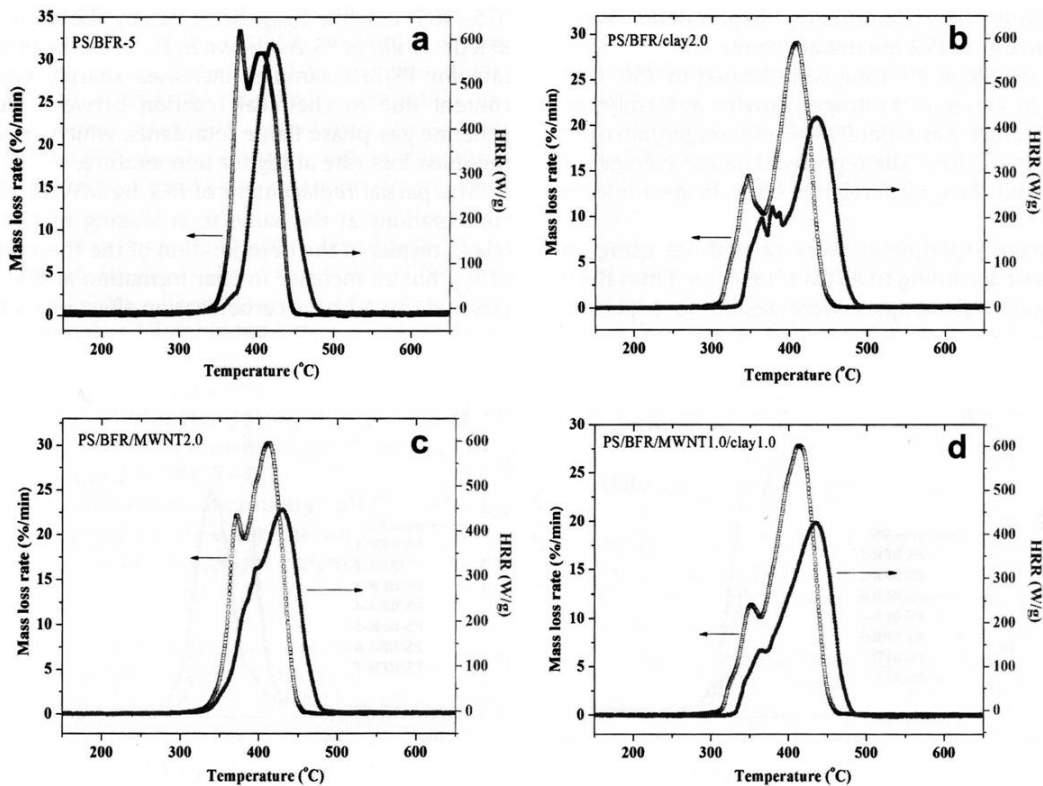


Fig. 4.: Comparison of some parameters tested by MCC for brominated flame retardant PS formulation. (Note: A1, A2,... ..D1 corresponds to PS/BFR-1, PS/BFR-2... ..PS/BFR/clay1.0/MWNT1.0, respectively.)

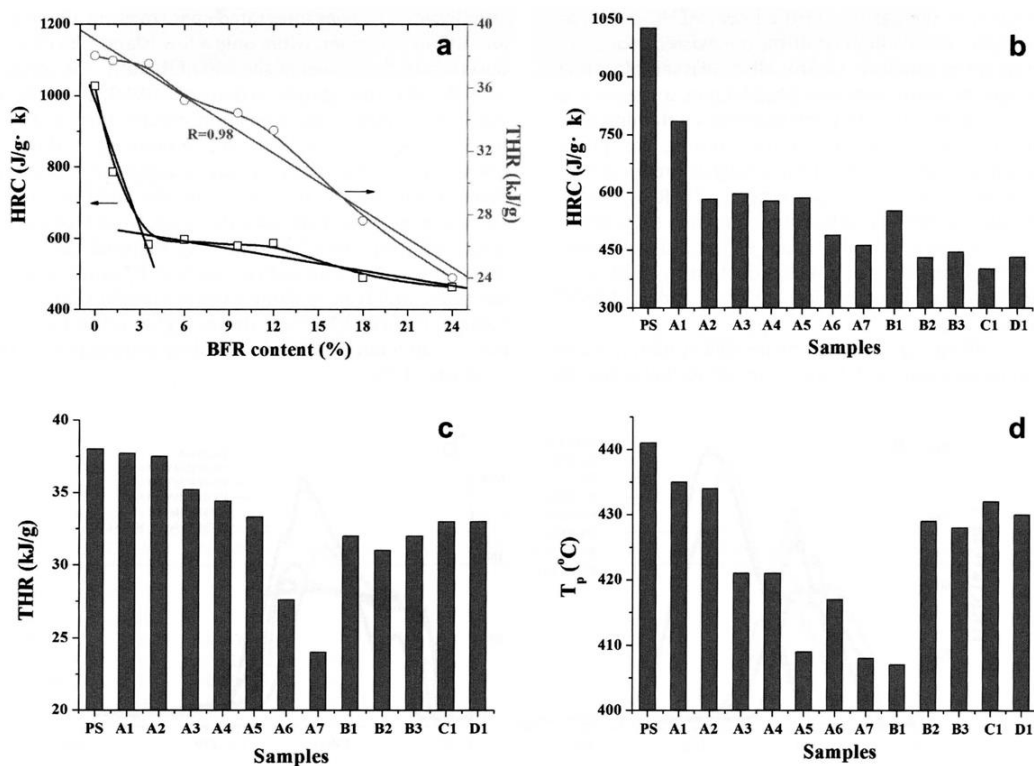


Fig. 5.: HRR curves of brominated flame retardant PS compounds in cone calorimetry.

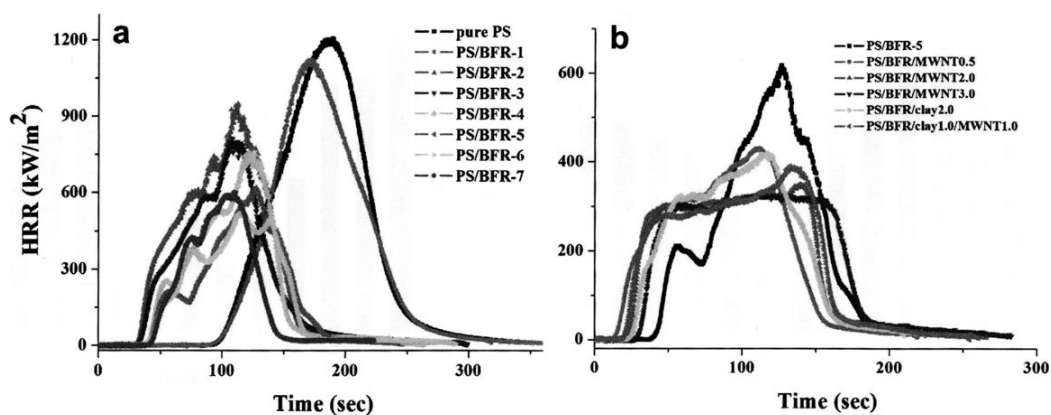


Fig. 6.: Photographs of collected char from (a) PS/BFR/clay2.0, and (b) PS/BFR/MWNT2.0.

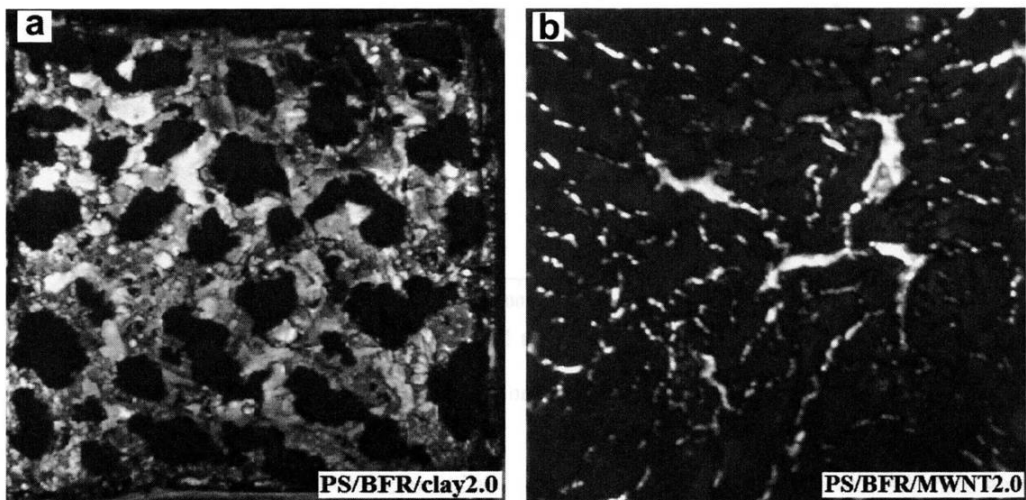


Fig. 7.: Comparison and correlations between MCC and Cone.

